JACS
JOURNAL OF THE AMERICAN CHEMICAL SOCIETY
Communication
pubs.acs.org/JACS

Exposing the Dynamics and Energetics of the N-Heterocyclic Carbene–Nanocrystal Interface

Haipeng Lu,[†] Zhaohui Zhou,[†,‡] Oleg V. Prezhdo,*[,†] and Richard L. Brutchey*[,†]

[†]Department of Chemistry, University of Southern California, Los Angeles, California 90089, United States

[‡]International Research Center for Renewable Energy, State Key Laboratory of Multiphase Flow in Power Engineering, Xi'an Jiaotong University, Xi'an 710049, China

Supporting Information

ABSTRACT: N-Heterocyclic carbenes (NHCs) are becoming increasingly popular ligand frameworks for nanocrystal surfaces; however, as of yet the nature of the NHC–nanocrystal interface remains unexplored across different material types. Here we report a facile synthetic route to NHC-stabilized metal and metal chalcogenide nanocrystals. It was observed that NHC–Ag nanocrystals are colloidally stable, but much less so than the corresponding NHC–Ag_2E analogues. Comprehensive NMR studies suggest a dynamic NHC–nanocrystal interface for both NHC–Ag and NHC–Ag_2S; however, density functional theory calculations reveal a much stronger binding affinity of the NHC ligands to Ag_2S compared with Ag nanocrystals, which explains the superior colloidal stability of the metal chalcogenides. This offers new insight into the surface chemistry of neutral L-type carbenes in colloidal nanocrystal chemistry.

N-Heterocyclic carbenes (NHCs) are an important class of neutral L-type ligands because of their structural diversity, chemical stability, and electron-rich σ-donating ability that leads to stable bonds with a wide swath of elements in the periodic table.[1] As a direct result of these characteristics, NHCs have been gradually gaining interest as ligands for the functionalization and stabilization of inorganic surfaces.[2] To this point, NHCs have been used as a supporting ligand framework for both colloidal metal nanocrystals (i.e., Au, Pd, Pt, and Ru NCs)[3] and planar Au surfaces.[4] As an example of their utility, NHC-functionalized Au surfaces have been shown to possess both enhanced thermal and chemical stability compared with thiol-functionalized ones.[4b,5] Additionally, NHC functionalization has recently been shown to have an important function in increasing the activity of Au NC electrocatalysts for the reduction of carbon dioxide.[6]

Despite the success and demonstrated utility of coupling NHC ligands with certain metal NCs, such as Au NCs, there has been comparatively less success in using NHCs to support NCs of other materials.[2,7] For example, while NHC-supported Au NCs are now well-known to possess good colloidal stability,[3a,b] there has heretofore been a noticeable absence of stable NHC–Cu and NHC–Ag NC congeners in the literature. Likewise, there has been scant mention in the literature of the application of NHCs to nonmetal NCs, such as covalent semiconductors,[8] even though other L-type ligands such as amines and phosphines are well-known to coordinate to and stabilize many semiconductor NCs.[9] Much of the current lack of material diversity for NHC-stabilized NCs stems from a lack of fundamental insight into the NHC–NC interface, which has not yet been studied across different surfaces.

In an effort to better understand the nature of the NHC–NC interface, in this work we developed a synthetic strategy for NHC-stabilized Ag and Ag_2E (E = S, Se) NCs in order to explore NHC ligand binding across both metal and covalent semiconductor NC surfaces. We observed an empirical difference in colloidal stability between the material platforms, which was explained in terms of NHC ligand dynamics and binding energies using a complement of solution NMR spectroscopy and density functional theory (DFT) calculations. This enabled the extension of this chemistry to the preparation of colloidal NHC–$Cu_{2-x}E$ NCs, where $0 < x \leq 1$, using NHC–Cu NC intermediates.

Bromo[1,3-(ditetradecyl)benzimidazol-2-ylidene]silver(I) was used as the NHC precursor to both NHC–Ag and NHC–Ag_2E NCs. This particular NHC has previously been employed to stabilize colloidal NHC–Au NCs.[3c] Colloidal NHC–Ag NCs were first obtained via a biphasic reduction of the NHC–AgBr complex with excess $NaBH_4$ in dichloromethane and water. The resulting NHC–Ag NCs were isolated from the organic phase and, upon purification, could be redispersed in nonpolar solvents. The lack of stable NHC–Ag NCs in the literature may be a result of the reduced bond dissociation energy of the NHC–Ag bonds compared with the NHC–Au bond.[10] As a direct consequence, NHC ligands may not be as effective at stabilizing Ag NCs since the dissociation of NHC ligands can result in NC aggregation. Therefore, to achieve colloidally stable NHC–Ag NCs, a lower concentration of the NHC–AgBr precursor was utilized to prevent subsequent aggregation of the resulting NCs.

The as-synthesized NHC–Ag NCs can be readily dispersed in nonpolar solvents such as toluene, tetrachloroethylene (TCE), and 1-octadecene (ODE) to give optically transparent dark-red colloidal suspensions that are stable for approximately 1 week. A characteristic localized surface plasmon resonance (LSPR) band from the NHC–Ag NCs centered at λ = 414 nm was observed by UV–vis absorption spectroscopy (Figure 1a). Powder X-ray diffraction (XRD) confirmed that the as-synthesized product crystallizes in the expected face-centered

Received: August 29, 2016
Published: October 28, 2016

DOI: 10.1021/jacs.6b09065
J. Am. Chem. Soc. 2016, 138, 14844–14847

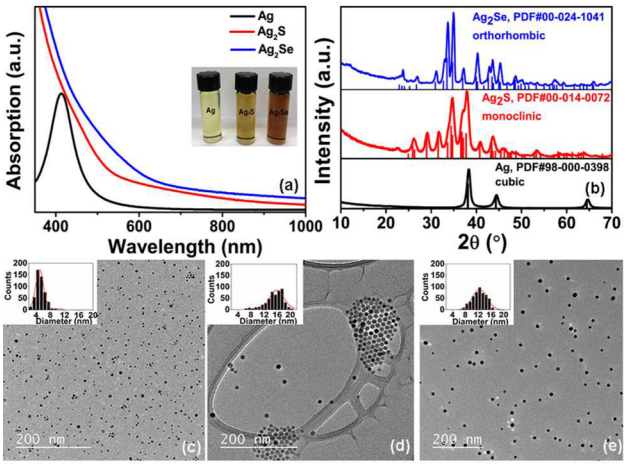

Figure 1. (a) UV−vis absorption spectra of NHC−Ag, NHC−Ag_2S, and NHC−Ag_2Se NC suspensions in toluene. The inset is a photograph of dilute toluene suspensions the NCs. (b) Powder XRD patterns of NHC−Ag, NHC−Ag_2S, and NHC−Ag_2Se NCs. (c−e) TEM micrographs of NHC-stabilized (c) Ag, (d) Ag_2S, and (e) Ag_2Se NCs. The insets are the size distributions of the corresponding NCs (n = 500 counts).

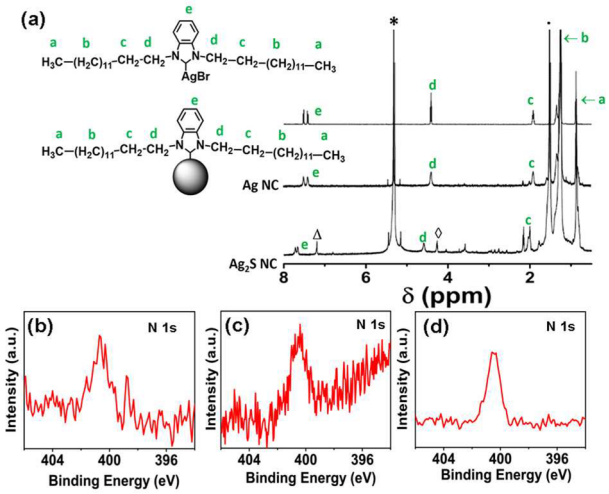

Figure 2. (a) ^{1}H NMR spectrum of NHC−AgBr, NHC−Ag NCs, and NHC−Ag_2S NCs. Resonances from 0.2 to 8 ppm are assigned accordingly. Solvent impurities are indicated by * (CH_2Cl_2), Δ (toluene), ◊ (ethanol), and ● (H_2O). (b−d) High-resolution N 1s XPS spectra of NHC−Ag, NHC−Ag_2S, and NHC−Ag_2Se NCs, respectively.

cubic (fcc) phase of Ag (Figure 1b). Transmission electron microscopy (TEM) analysis revealed the NHC−Ag NCs to be spherical in morphology with a mean diameter of 5.2 nm and standard deviation about the mean (σ/d) of 23% (Figure 1c). The size and size distribution of the NHC−Ag NCs can be readily tuned by changing the reagent concentrations; for example, if the concentrations of both NHC−AgBr and $NaBH_4$ are doubled, NHC−Ag NCs with a mean diameter of 9.0 nm (σ/d = 16%) can be achieved.

Subsequently, the NHC−Ag NCs were used as seeds for the synthesis of NHC−Ag_2E NCs. To avoid the introduction of additional extraneous ligands into the synthesis, the NHC−Ag NCs and S or Se were separately suspended/dissolved in a noncoordinating solvent (i.e., ODE). NHC−Ag_2E NCs were prepared by injecting the chalcogen in ODE into the NHC−Ag NC suspension at 120 °C. Absorption measurements displayed distinctive features into the near-IR for the NHC−Ag_2S and NHC−Ag_2Se NCs and confirmed the absence of the Ag LSPR band, indicating full conversion from Ag to Ag_2E NCs (Figure 1a). XRD patterns confirmed the purified NC products to be phase-pure monoclinic Ag_2S (PDF no. 00-014-0072) and orthorhombic Ag_2Se (PDF no. 00-024-1041) (Figure 1b). The stoichiometry of Ag_2S and Ag_2Se was confirmed by inductively coupled plasma−optical emission spectroscopy (ICP-OES), which gave a Ag/S ratio of 2.28 and a Ag/Se ratio of 2.11. TEM analysis showed spherical NCs with a mean diameter of 15.2 nm (σ/d = 17%) for Ag_2S and 12.4 nm (σ/d = 17%) for Ag_2Se NCs based on a 5.2 nm NHC−Ag NC seed (Figure 1d,e). Additionally, the colloidal stabilities of these NHC-stabilized Ag_2S and Ag_2Se NCs are excellent, with no noticeable aggregation or precipitation after >6 months.

To understand the marked difference in colloidal stability between the NHC-stabilized metal and covalent semiconductor surfaces, the colloidal NHC−Ag and NHC−Ag_2S NCs were interrogated as model systems using a battery of spectroscopic techniques. Solution ^{1}H NMR spectroscopy was applied to gain direct insight into the chemical identity of the surface ligands. The NHC−Ag NCs display an ^{1}H NMR spectrum similar to that of the NHC−AgBr precursor (Figure 2a), with a single set of benzimidazole and tetradecyl resonances. However, the observed broadening of these resonances for the NHC−Ag NCs results from slower tumbling of the ligands, indicating that the NHC is coordinated to the NC surface.[11] The same set of resonances was also observed for the NHC−Ag_2S NCs, with a slight downfield shift of all corresponding peaks (Figure 2a). Further proof follows from a direct comparison of the ^{1}H−^{13}C HSQC spectra of both NHC−AgBr and an NHC−Ag NC suspension (Figure S1 in the Supporting Information). The NHC−Ag NC HSQC cross-peaks indeed agree well with those of the corresponding NHC−AgBr complex. These spectral data collectively suggest that the NHC ligands coordinate to the surfaces of both the Ag and Ag_2S NCs.

To gain a more comprehensive picture of the NHC−NC interface, diffusion-ordered NMR spectroscopy (DOSY) was performed on suspensions of both purified NHC−Ag and NHC−Ag_2S NCs in $CDCl_3$ (Figure S2). Diffusion coefficients for the NHC ligands of 5.0×10^{-10} and 2.3×10^{-10} m^2/s were measured for Ag NCs and Ag_2S NCs, respectively. Both of these diffusion coefficients are smaller than that of the free NHC−AgBr complex, which exhibits a diffusion coefficient of 6.5×10^{-10} m^2/s. The hydrodynamic diameter of the NCs can be obtained from the diffusion coefficients (d_H) using the Stokes−Einstein equation;[11] however, the observed d_H of the NHC−Ag and NHC−Ag_2S NCs were only 1.7 and 3.7 nm, respectively, which are smaller than the expected core diameters of 5 and 15 nm based on TEM. This thus suggests a dynamic NHC−NC interface with an equilibrium between bound and free NHC ligands. As a result, a weighted mean diffusion coefficient between the bound and unbound NHC ligands was observed.[12] On this basis, NHC ligands on the surfaces of both Ag and Ag_2S NCs appear to be labile; however, this does not explain the observed difference in colloidal stability between the Ag and Ag_2S NCs.

The surface chemistry of the NHC−NCs was further corroborated by X-ray photoelectron spectroscopy (XPS), which showed the presence of N on the surface of the NHC−Ag, NHC−Ag_2S, and NHC−Ag_2Se NCs through a N 1s peak at a binding energy of ∼400.5 eV (Figure 2b−d). Interestingly, Br

DOI: 10.1021/jacs.6b09065
J. Am. Chem. Soc. 2016, 138, 14844−14847

was revealed to be present in only the NHC−Ag NCs (as had been previously observed for NHC−Au NCs[3a]) but not in the case of the NHC−Ag_2S or NHC−Ag_2Se NCs (Figure S3). The atomic Br/Ag ratio was quantified by XPS to be <14% for the NHC−Ag NCs, and thus, the surface is not expected to be entirely shelled with Br. This degree of surface Br does, however, suggest that Br plays a role at the surface of the Ag NCs, while only covalent NHC−Ag(I) interactions are present in the NHC−Ag_2E NCs. Moreover, the presence of Br in the NHC−Ag NCs is not associated with protonated benzimidazolium bromide since a proton resonance at ∼11.6 ppm was not observed in the ^{1}H NMR spectrum of the NCs. The quantities of NHC on the NC surfaces were determined by thermogravimetric analysis (Figure S4), with the mass loss at ∼320 °C assigned to the loss of NHC ligands.[13] The NHC−Ag and NHC−Ag_2E NCs display a single-step mass loss event at ∼320 °C of 40%, 3.4%, and 8.6% for NHC−Ag, NHC−Ag_2S, and NHC−Ag_2Se NCs, respectively. The numbers of NHC ligands per NC could then be estimated assuming a spherical morphology for Ag (5 nm), Ag_2S (15 nm), and Ag_2Se (12 nm) NCs to be 603, 530, and 825, respectively. These values are all below the reported surface density previously reported for 4 nm NHC−Au NCs (∼730 ligands per NC).[13]

Since the dynamic nature of the NHC−NC interface does not appear to be the origin of the difference in colloidal stability between the Ag and Ag_2E NCs, we investigated potential differences in binding energy. The binding energies of a model 1,3-(dimethyl)benzimidazol-2-ylidene NHC ligand to ∼1.2 nm clusters of Ag and Ag_2S were calculated using DFT. Because of the experimentally observed presence of Br in the Ag NCs, we modified the Ag cluster surface with Br atoms. The calculations revealed that the binding interaction between the NHC and the Br-modified Ag cluster is weak. The NHC molecule could only bind to the vertex site on the surface of the Ag cluster with a small binding energy of 0.30 eV (Figure 3a). The vertex site of the Ag NC is least coordinated, providing the best opportunity for ligand binding. For the other two binding sites, namely, the face-centered and ridge sites, the NHC failed to bind to the surface of the Ag cluster, with negligible binding energies and large distances between the coordinating C atom in NHC and the Ag atom on the cluster (Figure 3b,c). This may be attributed to steric hindrance between the alkyl groups in the NHC and the surface Br. The calculated Bader charge in the vertex site shows that the electron charge is transferred from surface Ag to Br, giving about 0.43 e/Br atom (Table S1 in the Supporting Information). Accordingly, a weak modification of the C orbitals is observed in the valence band of the density of states (DOS). In comparison, the NHC ligand binds to the Ag_2S cluster through relatively strong bonding interactions between the carbene C and Ag^+ cations on the surface of the cluster. The geometries and binding energies for three types of binding of the NHC to the Ag_2S cluster are similar (Figure 3d−f), suggesting similar local environments for the Ag atoms on the surface. The binding energy varies from 0.57 to 0.77 eV for the three binding geometries, with the C−Ag bond length decreasing from 2.47 to 2.26 Å, respectively. The relatively strong binding of the NHC to the Ag_2S cluster is also reflected in the DOS for the geometry of binding site 2, where a strong modification of the C orbitals is observed in the valence band. It is noteworthy that surface passivation by NHC ligands does not appear to introduce any mid-gap trap states in the Ag_2S cluster since the orbitals of the NHC ligands appear only in the valence or conduction bands. Therefore, as a strong σ donor,

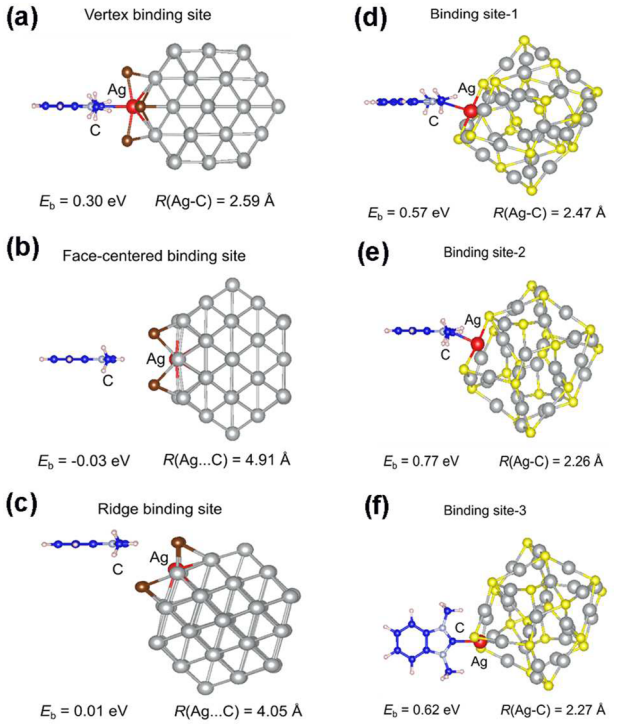

Figure 3. Geometries and binding energies for three types of binding of an NHC ligand to (a−c) a Ag cluster that was decorated with four Br atoms surrounding the binding site and (d−f) a Ag_2S cluster. Ag, S, Br, H, C, and N atoms are depicted in gray, yellow, brown, pink, deep blue, and light blue, respectively. The red Ag atom denotes the surface binding site for the NHC ligand.

the neutral NHC ligands not only provide strong binding to the Ag_2S NCs to impart excellent colloidal stability but also present the possibility to positively affect the optoelectronic properties of covalent semiconductor NCs.

Furthermore, the same chemistry was extended to NHC−CuBr to generate well-defined NHC−$Cu_{2-x}E$ NCs ($0 < x \leq 1$; see the Supporting Information). The reduced product from NHC−CuBr was shown to be fcc Cu NCs, which possess limited oxidative and colloidal stability. Subsequent DFT calculations showed a very weak binding interaction between the NHC ligand and an analogous Cu cluster decorated with Br (Figure S9). After dispersion of the NHC−Cu NCs in ODE, colloidal NHC−$Cu_{2-x}E$ NCs were prepared following the same reaction procedure as before. Interestingly, varying the nominal chalcogen stoichiometry in the reaction allowed for control over the copper chalcogenide phase. For instance, hexagonal NHC−CuE NCs were produced when the chalcogen was added in a Cu/E molar ratio of 1:1, while cubic NHC−$Cu_{1.8}E$ NCs were obtained with a Cu/E molar ratio of 2:1. The addition of this NHC−MBr precursor chemistry to give NHC−Cu and NHC−$Cu_{2-x}E$ NCs further extends the generality of this approach in generating new metal and covalent semiconductor NCs that are coordinated by NHC ligands. As with their Ag counterparts, the NHC−$Cu_{2-x}E$ NCs possess superior colloidal stability compared with the NHC−Cu NC intermediates.

We have successfully demonstrated the synthesis of colloidally stable NHC-stabilized Ag metal and Ag_2E metal chalcogenide NCs using a bromo[1,3-(ditetradecyl)-benzimidazol-2-ylidene]silver(I) synthon. With a combination of ^{1}H NMR, HSQC, and DOSY spectra, a dynamic

DOI: 10.1021/jacs.6b09065
J. Am. Chem. Soc. 2016, 138, 14844−14847

coordination sphere of effective but labile NHC ligands was found to coordinate to both Ag and Ag_2S NCs, with the Ag_2S NCs observed to be more colloidally stable with respect to time. This empirical difference is rationalized to be a result of the different binding energies between the NHC ligand and the NC surface for the two materials, with a significantly larger binding affinity between the NHC and Ag_2S NCs revealed by DFT calculations. These experimental and computational results help elucidate a more comprehensive understanding of the NHC−NC interface, providing new insight into the surface chemistry of colloidal NCs with L-type NHC ligands across a range of materials. The excellent colloidal stability of NHC−$M_{2-x}E$ NCs and the implications of strong σ donation with respect to their optoelectronic properties suggest that these are promising ligands to be further explored for the stabilization of covalent semiconductor NCs.

■ ASSOCIATED CONTENT

Supporting Information

The Supporting Information is available free of charge on the ACS Publications website at DOI: 10.1021/jacs.6b09065.

Experimental procedures, TGA traces, FT-IR spectra, photographs, TEM images, XPS spectra, DFT calculation details, and NMR spectra (PDF)

■ AUTHOR INFORMATION

Corresponding Authors

*prezhdo@usc.edu

*brutchey@usc.edu

Notes

The authors declare no competing financial interest.

■ ACKNOWLEDGMENTS

This chemistry and surface characterization were developed with funding support from the National Science Foundation under DMR-1506189 to R.L.B. The DFT calculations were performed with funding from the National Science Foundation under CHE-1565704 to O.V.P. O.V.P. is also grateful to the Photochemistry Center of the Russian Science Foundation, project No. 14-43-00052, for hospitality during manuscript preparation.

■ REFERENCES

(1) Hopkinson, M. N.; Richter, C.; Schedler, M.; Glorius, F. *Nature* **2014**, *510*, 485−496.

(2) Zhukhovitskiy, A. V.; MacLeod, M. J.; Johnson, J. A. *Chem. Rev.* **2015**, *115*, 11503−11532.

(3) (a) Vignolle, J.; Tilley, T. D. *Chem. Commun.* **2009**, 7230−7232. (b) Song, S. G.; Satheeshkumar, C.; Park, J.; Ahn, J.; Premkumar, T.; Lee, Y.; Song, C. *Macromolecules* **2014**, *47*, 6566−6571. (c) Ling, X.; Roland, S.; Pileni, M.-P. *Chem. Mater.* **2015**, *27*, 414−423. (d) Ranganath, K. V. S.; Kloesges, J.; Schäfer, A. H.; Glorius, F. *Angew. Chem., Int. Ed.* **2010**, *49*, 7786−7789. (e) Lara, P.; Rivada-Wheelaghan, O.; Conejero, S.; Poteau, R.; Philippot, K.; Chaudret, B. *Angew. Chem., Int. Ed.* **2011**, *50*, 12080−12084. (f) Baquero, E. A.; Tricard, S.; Flores, J. C.; de Jesús, E.; Chaudret, B. *Angew. Chem., Int. Ed.* **2014**, *53*, 13220−13224.

(4) (a) Zhukhovitskiy, A. V.; Mavros, M. G.; Van Voorhis, T.; Johnson, J. A. *J. Am. Chem. Soc.* **2013**, *135*, 7418−7421. (b) Crudden, C. M.; Horton, J. H.; Ebralidze, I. I.; Zenkina, O. V.; McLean, A. B.; Drevniok, B.; She, Z.; Kraatz, H.-B.; Mosey, N. J.; Seki, T.; Keske, E. C.; Leake, J. D.; Rousina-Webb, A.; Wu, G. *Nat. Chem.* **2014**, *6*, 409−414.

(5) Ling, X.; Schaeffer, N.; Roland, S.; Pileni, M.-P. *Langmuir* **2015**, *31*, 12873−12882.

(6) Cao, Z.; Kim, D.; Hong, D.; Yu, Y.; Xu, J.; Lin, S.; Wen, X.; Nichols, E. M.; Jeong, K.; Reimer, J. A.; Yang, P.; Chang, C. J. *J. Am. Chem. Soc.* **2016**, *138*, 8120−8125.

(7) Ling, X.; Schaeffer, N.; Roland, S.; Pileni, M.-P. *Langmuir* **2013**, *29*, 12647−12656.

(8) Aslanov, L.; Zakharov, V.; Zakharov, M.; Kamyshny, A.; Magdassi, S.; Yatsenko, A. *Russ. J. Coord. Chem.* **2010**, *36*, 330−332.

(9) Brutchey, R.; Hens, Z.; Kovalenko, M. V. *Chemistry of Organo-Hybrids: Synthesis and Characterization of Functional Nano-Objects*; Charleux, B., Copéret, C., Lacôte, E., Eds.; John Wiley & Sons: Hoboken, NJ, 2015; Chapter 7.

(10) Jacobsen, H.; Correa, A.; Poater, A.; Costabile, C.; Cavallo, L. *Coord. Chem. Rev.* **2009**, *253*, 687−703.

(11) Hens, Z.; Martins, J. C. *Chem. Mater.* **2013**, *25*, 1211−1221.

(12) (a) Grisorio, R.; Debellis, D.; Suranna, G. P.; Gigli, G.; Giansante, C. *Angew. Chem., Int. Ed.* **2016**, *55*, 6628−6633. (b) De Roo, J.; Ibáñez, M.; Geiregat, P.; Nedelcu, G.; Walravens, W.; Maes, J.; Martins, J. C.; Van Driessche, I.; Kovalenko, M. V.; Hens, Z. *ACS Nano* **2016**, *10*, 2071−2081.

(13) MacLeod, M. J.; Johnson, J. A. *J. Am. Chem. Soc.* **2015**, *137*, 7974−7977.

DOI: 10.1021/jacs.6b09065
J. Am. Chem. Soc. 2016, 138, 14844−14847